



UNIVERSIDADE D
COIMBRA

FACULDADE
DE CIÊNCIAS
E TECNOLOGIA



Evaluating the influence of the deformation of the forming tools in the thickness distribution along the wall of a cylindrical cup

M C Oliveira¹, D M Neto¹, A.F.G. Pereira¹, J L Alves² and LF Menezes¹

¹ University of Coimbra, CEMMPRE, Department of Mechanical Engineering, Portugal

² University of Minho, CMEMS, Department of Mechanical Engineering, Portugal



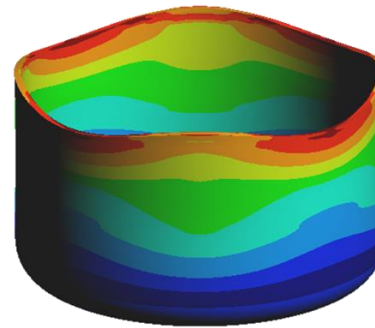
Introduction

Cylindrical cup forming

- **Anisotropic behavior** of the metallic sheets leads to the formation of **ears** in cylindrical cups
- **Earing profile** mainly dictated by the in-plane distribution of both the **r -values** and **yield stresses** (compression stress state)
- This was one of the challenges of ESAFORM 2021 Benchmark: EXACT



Experimental*



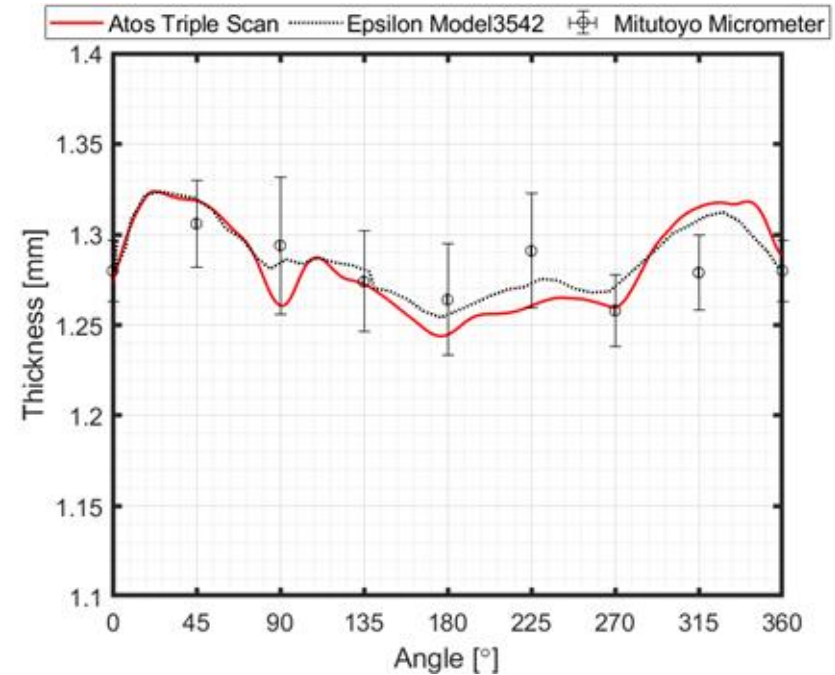
Simulation

*Anne Marie Habraken, Toros Arda Aksen, José L. Alves, Rui L. Amaral, Ehssen Betaieb, Nitin Chandola, Luca Corallo, Daniel J. Cruz, Laurent Duchêne, Bernd Engel, Emre Esener, Mehmet Firat, Peter Frohn-Sørensen, Jesús Galán-López, Hadi Ghiabakloo, Leo Kestens, Junhe Lian, Rakesh Lingam, Wencheng Liu, Jun Ma, Luís F. Menezes, Tuan Nguyen-Minh, Sara S. Miranda, Diogo M. Neto, André F.G. Pereira, Pedro A. Prates, Jonas Reuter, Benoit Revil-Baudard, Carlos Rojas-Ulloa, Bora Sener, Fuhui Shen, Albert Van Bael, Patricia Verleysen, Analysis of ESAFORM 2021 cup drawing benchmark of an Al alloy, critical factors for accuracy and efficiency of FE simulations, International Journal of Material Forming, Accepted to be published.

Introduction

Cylindrical cup forming

- If the thickness of the drawn flange is larger than the gap between the punch and the die, **cup wall ironing** will occur
- The ironing forces can lead to significant **elastic deformation of the forming tools** (punch and die)



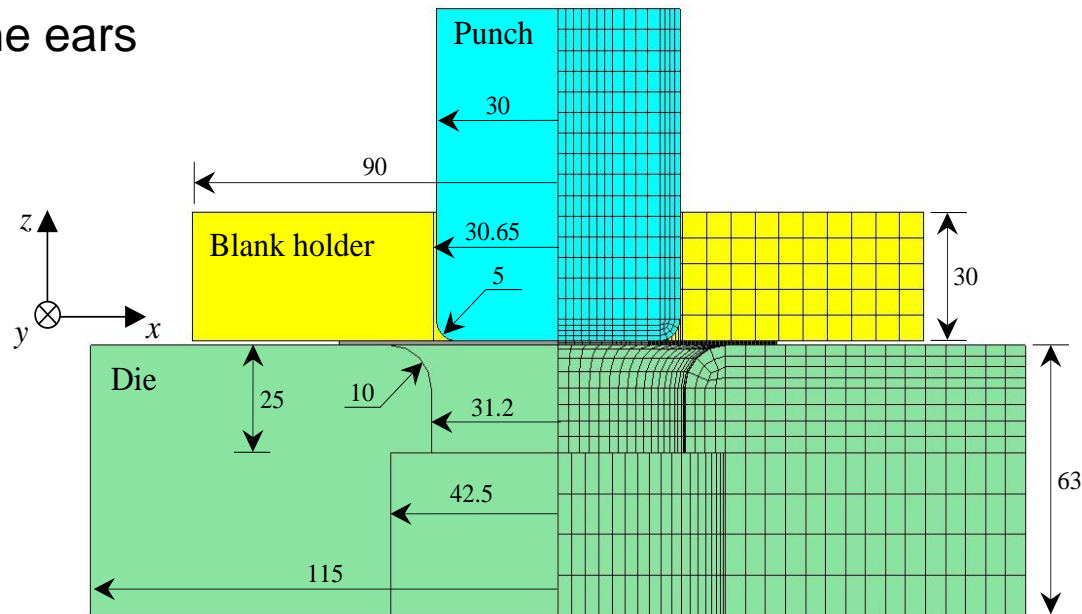
Thickness evolution for a cup height of 30 mm, using three methods.*

- **Objective:** Evaluate numerically the **deformation of the forming tools** during the deep drawing-ironing process of a cylindrical cup

Numerical models

Deep drawing of a cylindrical cup

- Aluminum alloy **AA6016-T4** sheet with 107.5 mm of diameter 0.98 mm of thickness
- Punch displacement of 60 mm (**full drawing**) and a constant blank holder force of 40 kN. A stopper with the same thickness of the blank was used to avoid the pinching of the ears

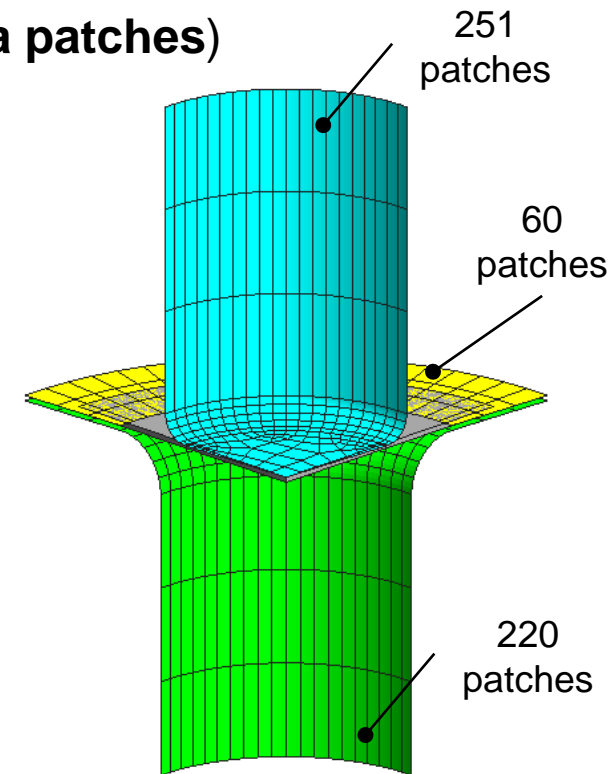
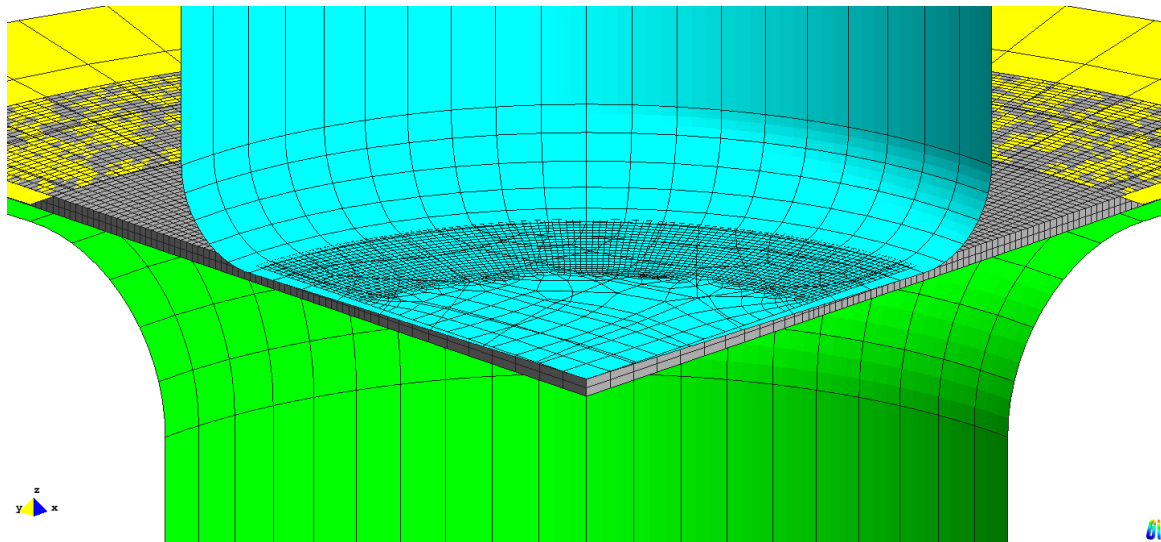


Schematic representation of the forming tools including main dimensions [mm] and the mesh adopted when considering deformable tools.

Numerical models

Finite element model: rigid tools

- **DD3IMP** in-house finite element code (implicit time integration)
- **1/4** of the model (symmetry conditions)
- Forming tools are assumed rigid (discretized by **Nagata patches**)
- Classical **Coulomb friction law**

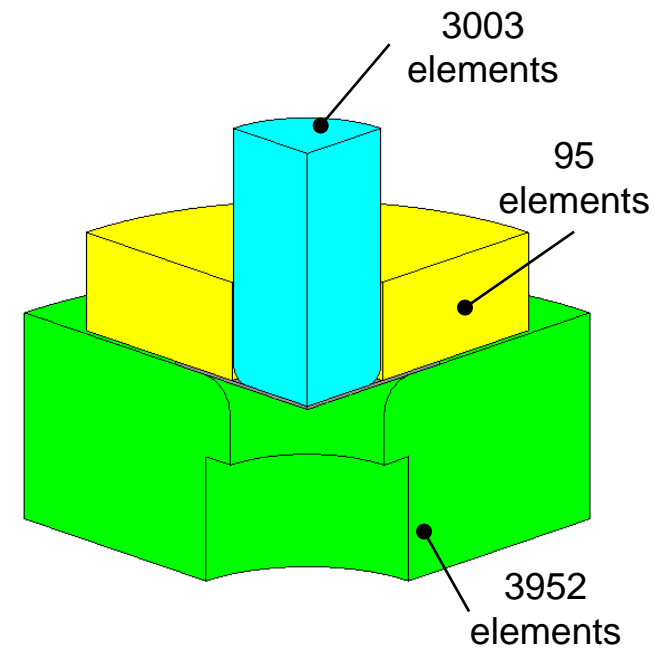
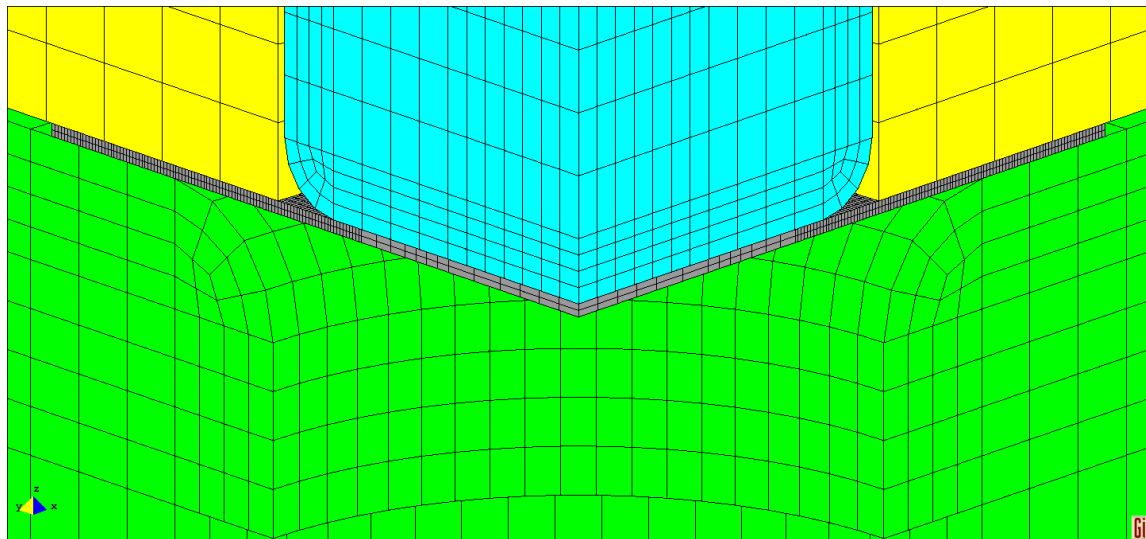


Rigid forming tools described with Nagata patches and blank discretization with 3D 8-node hexahedral finite elements (15408 elements; 16006 nodes).

Numerical models

Finite element model: deformable tools

- Forming tools are assumed solid (**3D 8-node hexahedral finite elements**).
Coarse discretization due to the use of Nagata patches surface smoothing
- The blank holder is controlled with an imposed displacement that increases linearly with the punch displacement, until a maximum value of 0.17 mm



Deformable forming tools described with solid elements and blank discretization with 3D 8-node hexahedral finite elements (15408 elements; 16006 nodes).

Numerical models

Constitutive models: blank

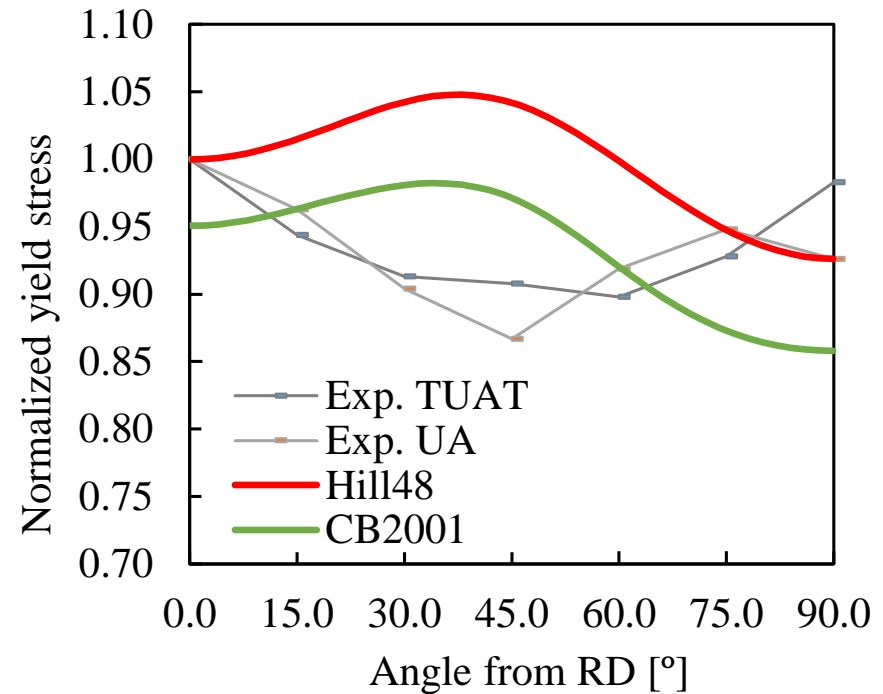
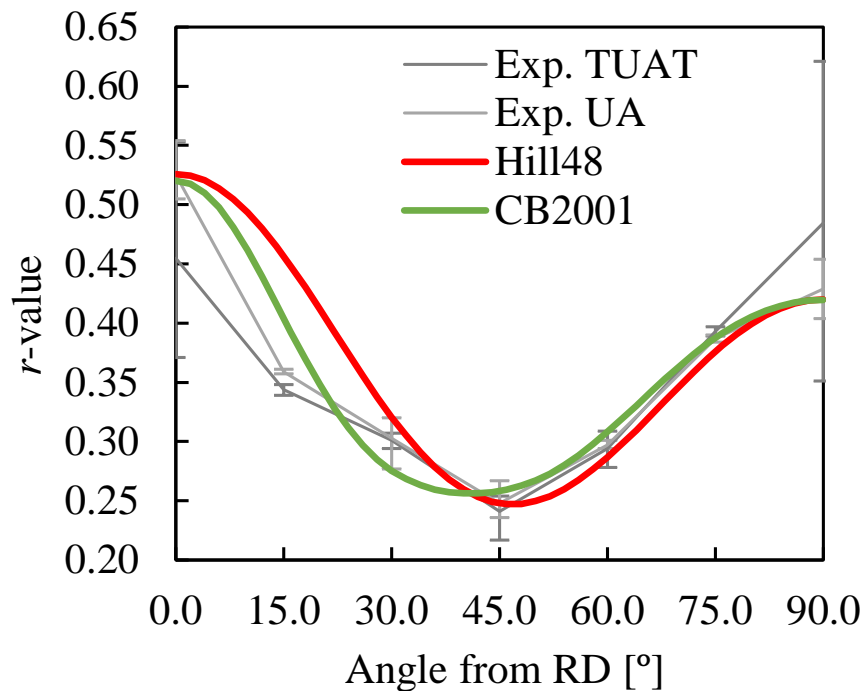
- Isotropic **elastic behavior** ($E=69$ GPa and $\nu=0.30$)
- Anisotropic **plastic behavior**:
 - ✓ Isotropic work hardening described by the **Swift law**
 - ✓ Orthotropic behavior modelled by the yield criteria **Hill48** and **CB2001**

- Set of experimental data used in the **calibration of the anisotropy parameters of CB2001**:
 - i. In-plane distribution of yield stress and r -values extracted from uniaxial tensile tests (every 15° to RD) performed by University of Aveiro (UA)*
 - ii. Data from cruciform biaxial tensile tests performed by Tokyo University of Agriculture and Technology (TUAT) *

Numerical models

Constitutive models: blank

- Both yield criteria lead to a similar in-plane evolution of the r -values and an identical trend for the normalized yield stress; both yield criteria **describe well the experimental r -values but are unable to capture the yield stress distribution**

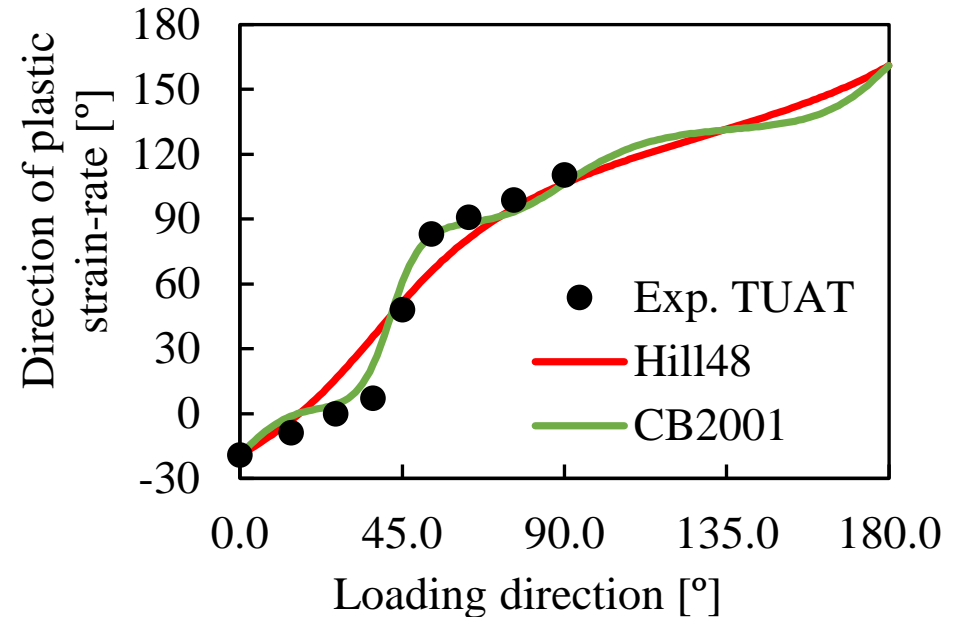
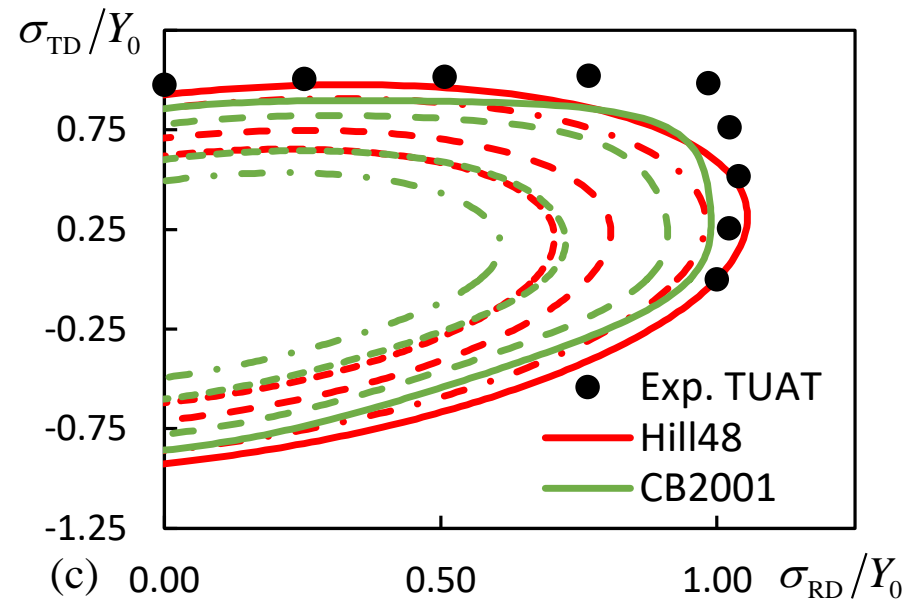


Comparison between experimental and predicted: (left) r -values; (right) yield stresses.

Numerical models

Constitutive models: blank

- Both yield surfaces present quite different descriptions of the **shear stresses**
- The direction of plastic strain-rate is also quite different for both yield criteria, since the CB2001 is much more flexible

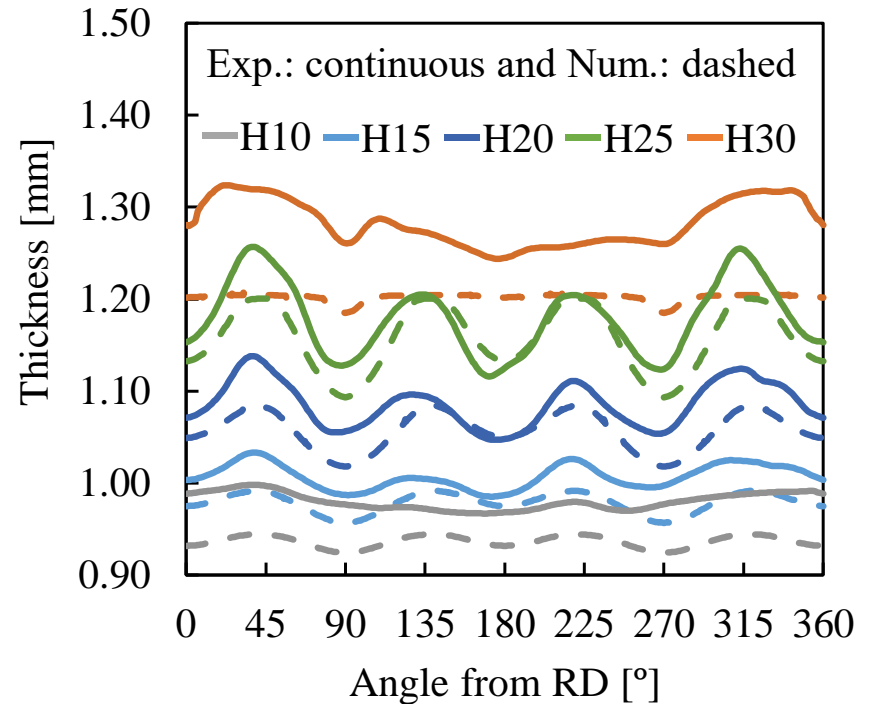
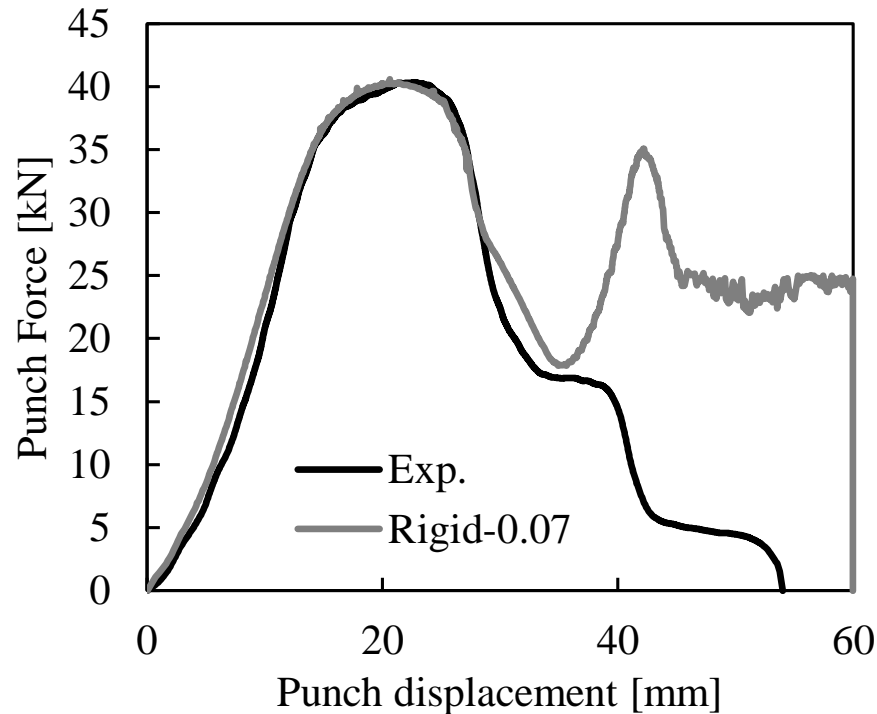


Comparison between experimental and predicted: (left) r -values; (right) yield stresses.

Results and discussion

Rigid tools

- The constant friction value of 0.07 enables an accurate description of the drawing force, but the ironing force is clearly overestimated. The thickness distribution is clearly underestimated

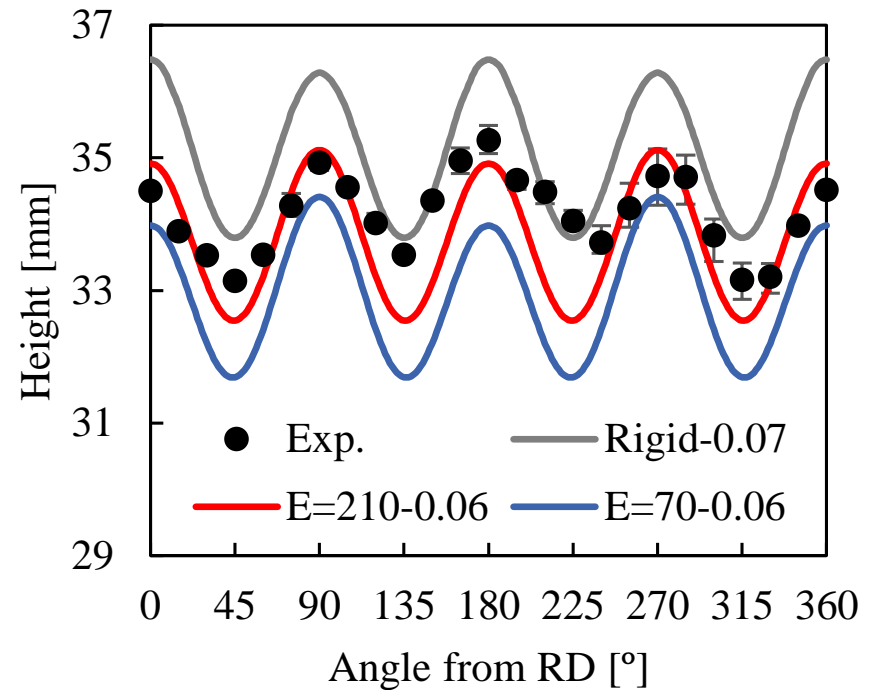
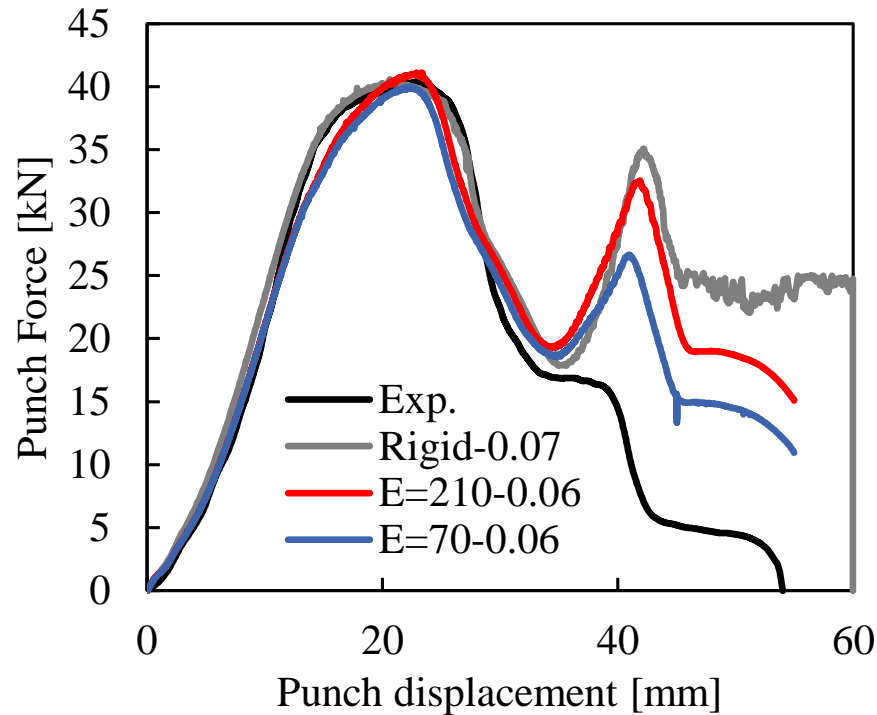


Comparison between experimental and predicted results using rigid tools, Hill'48 and $\mu=0.07$: (left) punch force-displacement and (right) thickness distribution along the cup circumference at different heights $H = 10, 15, 20, 25$ and 30 mm from the cup bottom

Results and discussion

Deformable tools: stiffness

- In the ironing stage, the punch force reduces with the decrease of the tools stiffness. The tools stiffness influences the cup height, i.e. the **average cup height decreases with the decrease of the tools stiffness**

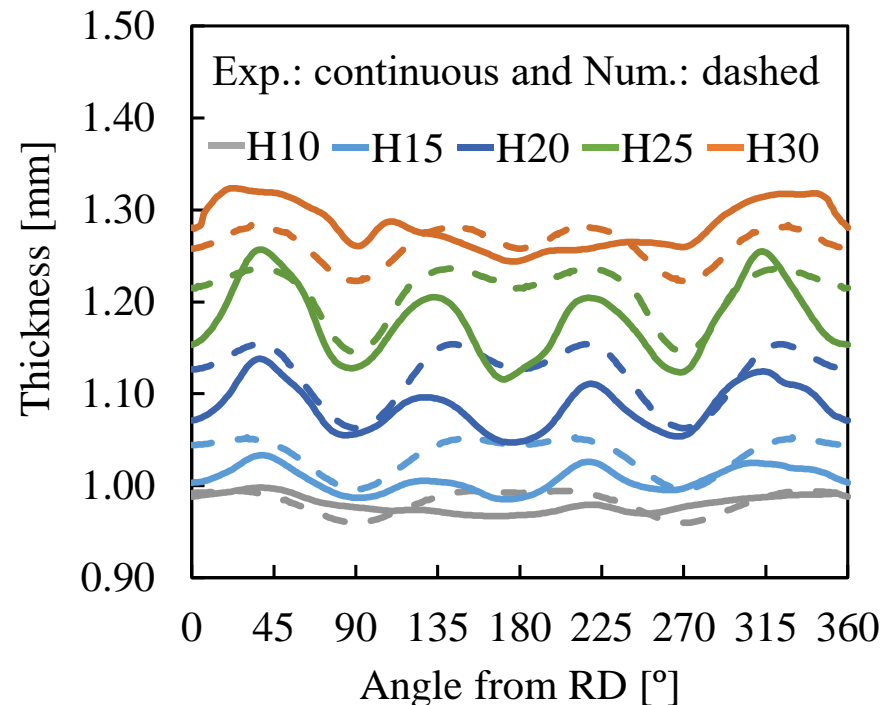
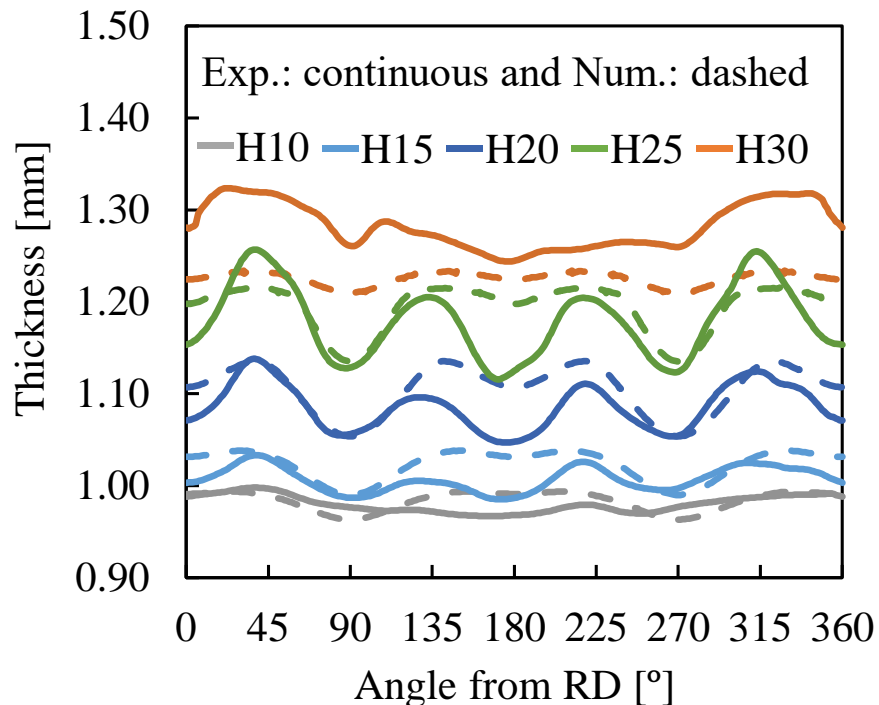


Comparison between experimental and predicted results using Hill'48 with rigid and deformable tools: (left) punch force-displacement and (right) earing profile.

Results and discussion

Deformable tools: stiffness

- A lower tool stiffness generates lower friction forces, contributing to a smaller cup with **higher thickness values** for the same height of the cup

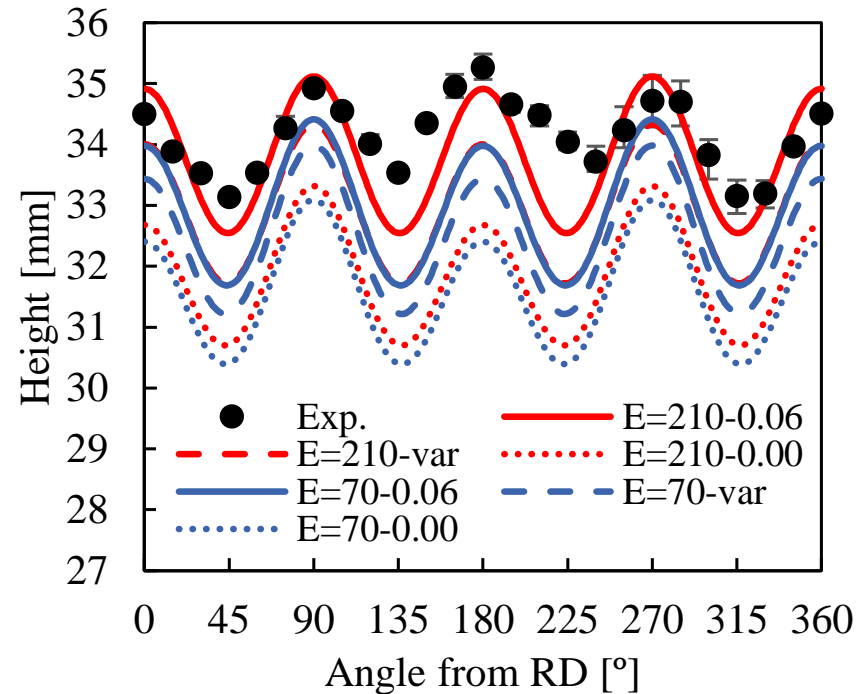
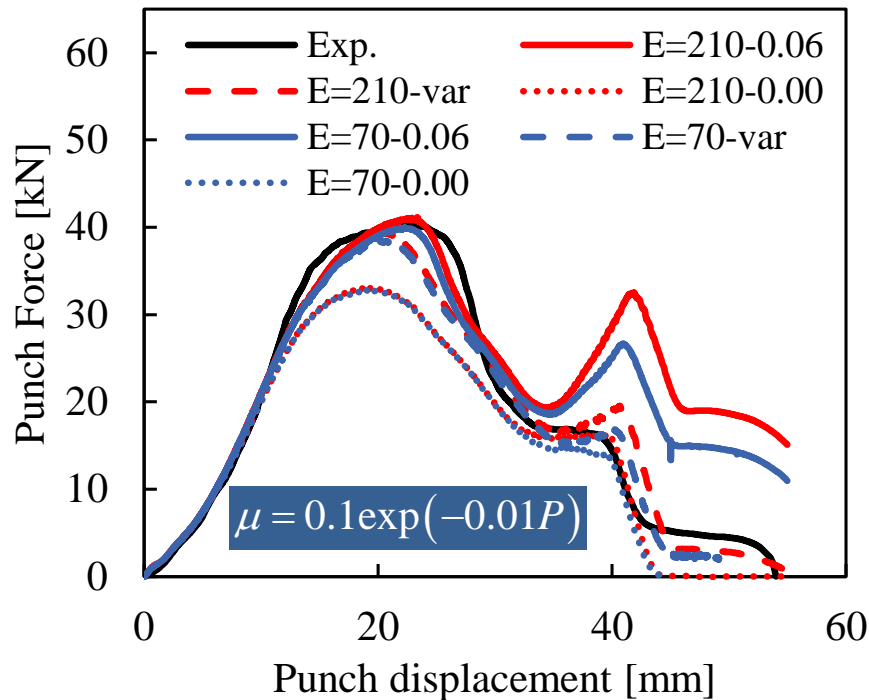


Comparison between experimental and predicted results using Hill'48 and deformable tools with $\mu=0.06$, for the distribution of the thickness along the cup circumference at different heights: (left) $E=210$ GPa and (right) $E=70$ GPa..

Results and discussion

Deformable tools: friction law

- The evolutionary friction law enables a more accurate global description of the punch force for **both the drawing and the ironing stages**, due to the reduction of the friction value with the increase of the contact pressure

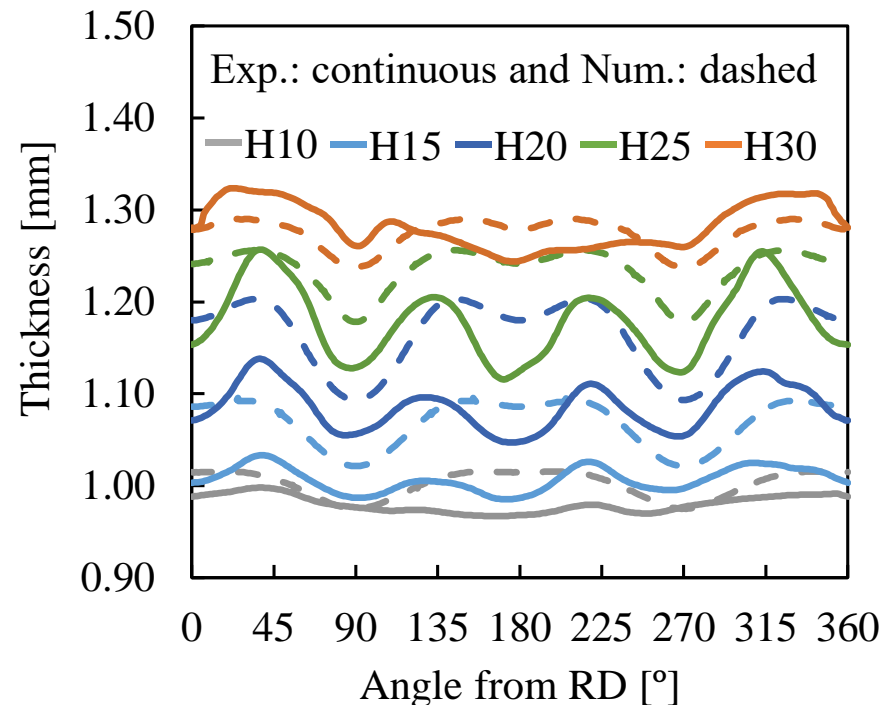
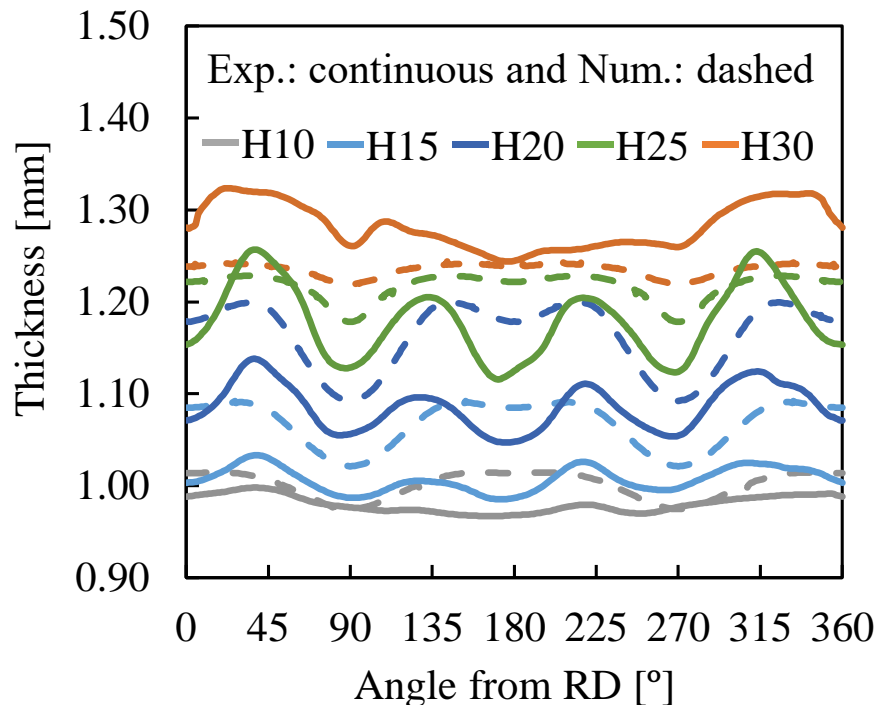


Comparison between experimental and predicted results using Hill'48, deformable tools and different values for the friction coefficient: (left) punch force-displacement and (right) earring profile.

Results and discussion

Deformable tools: friction law

- The average thickness in the cup wall increases with the decrease of the friction coefficient and the change is not uniform along the circumferential coordinate

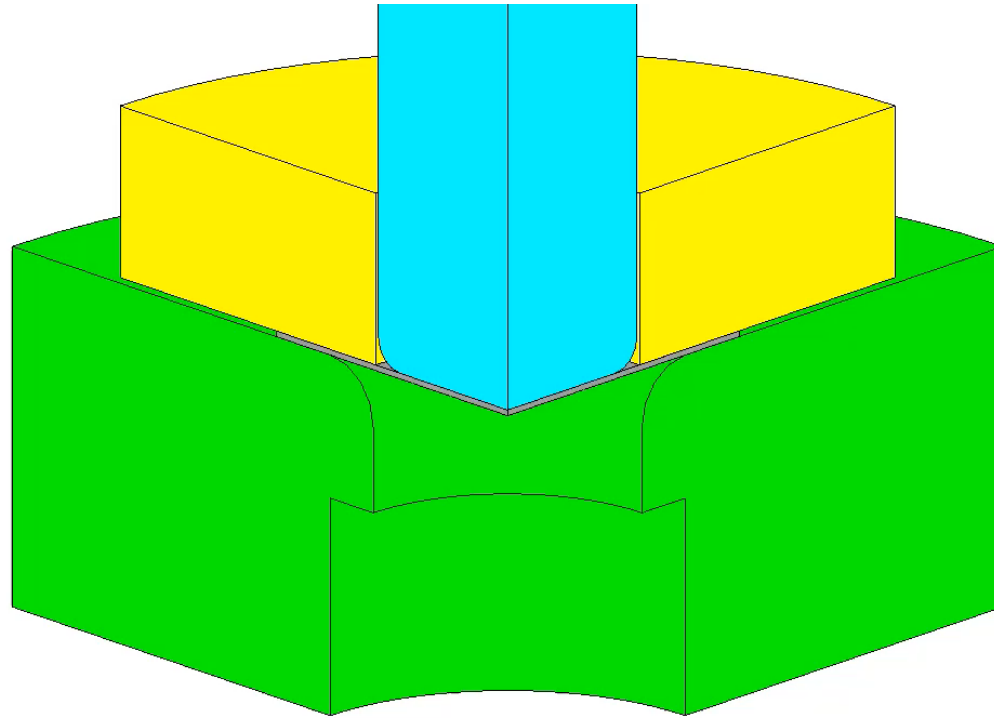


Comparison between experimental and predicted results using Hill'48, deformable tools and a null friction coefficient, for the evolution of the thickness along the cup circumference at different heights: (left) $E=210$ GPa and (right) $E=70$ GPa.

Results and discussion

Deformable tools: friction law

- The impact of the tools stiffness is mainly observed on the **top of the vertical wall of the cup** and its dictated by the gap (between the punch and the die) and the increase of thickness in the flange area

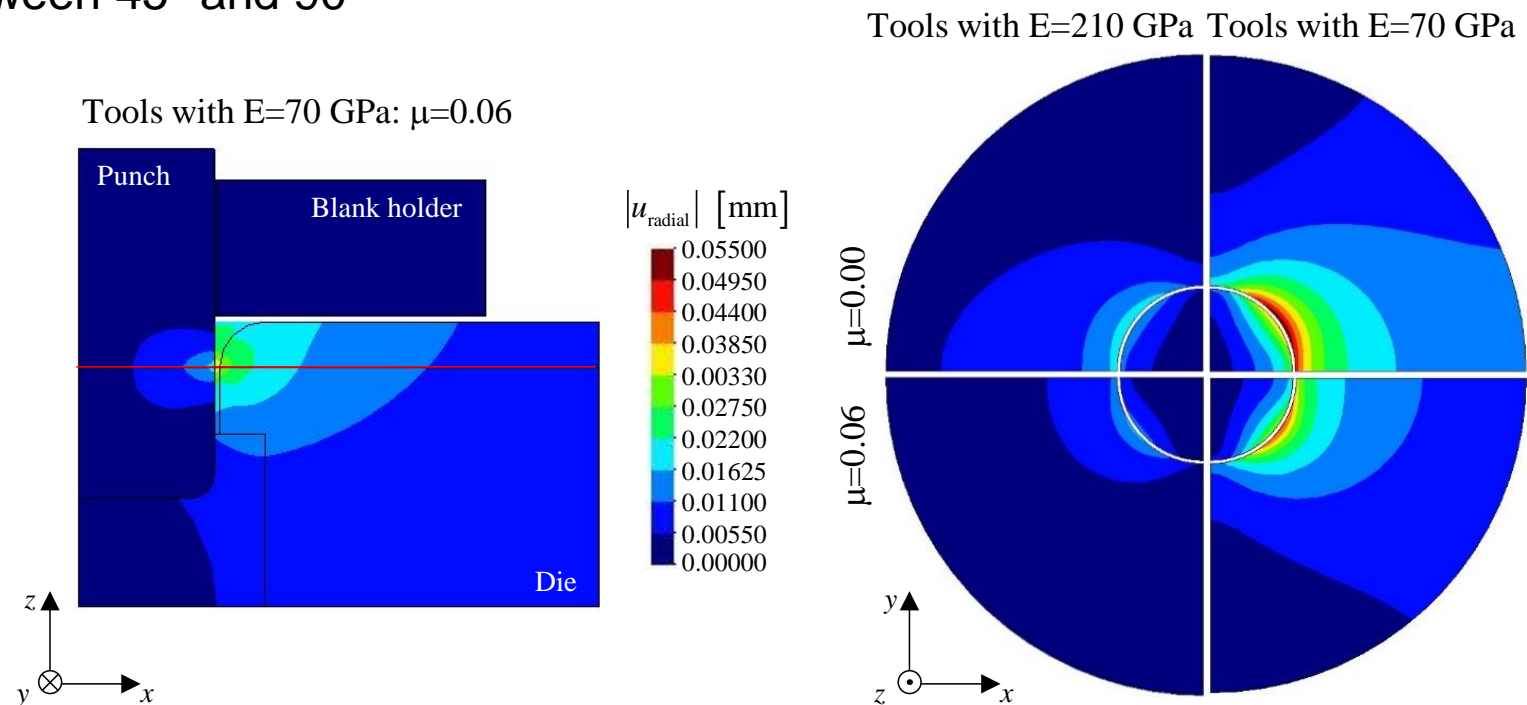


Evolution of the equivalent stress predicted using Hill'48 and deformable tools with $\mu=0.06$ and $E=210$ GPa.

Results and discussion

Deformable tools: friction law

- The tools deflection is higher between 0° and 45° to RD, i.e. where there is a greater thickening of the blank, which is related with the lower r -value observed between 45° and 90°

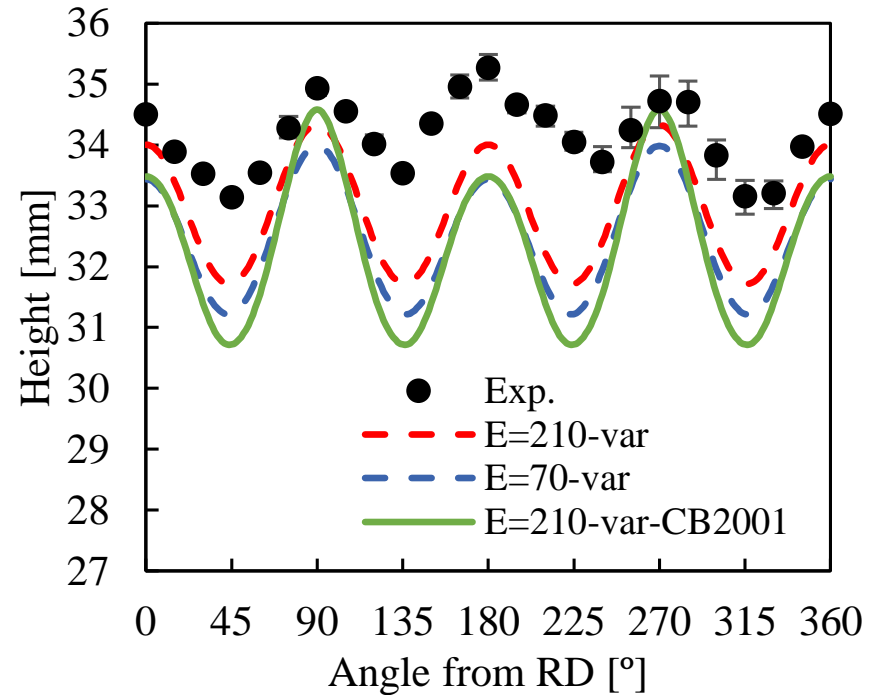
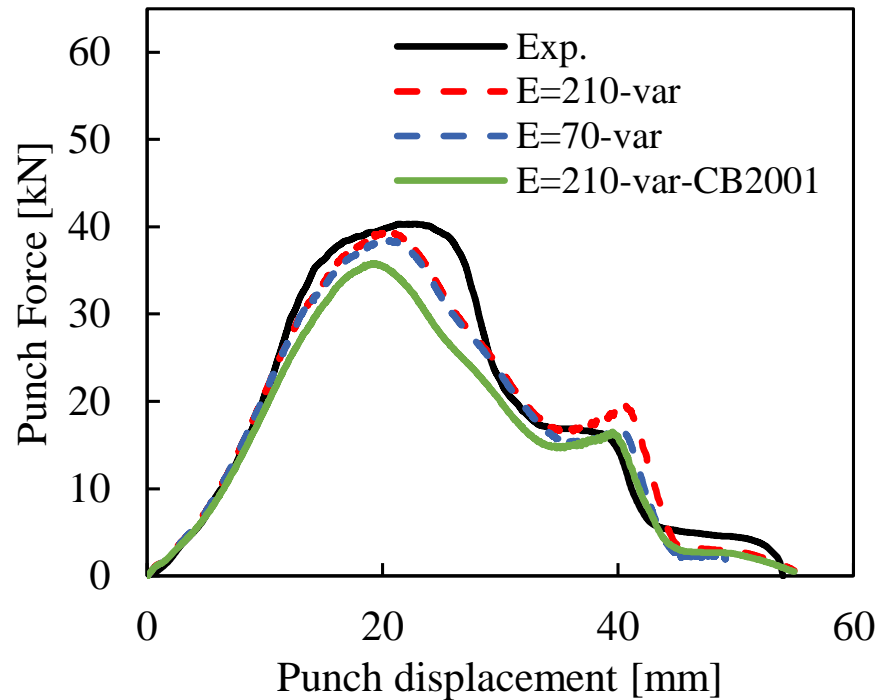


Contour plot of the norm of the radial nodal displacements [mm] in the tools for a punch displacement of 40 mm: (left) for the less stiff tools and (right) for both deformable tools and constant friction coefficient values, in the plane marked with the red line in the left.

Results and discussion

Deformable tools: yield criteria

- The punch force predicted with the CB2001 is slightly lower than the one observed with the Hill'48, since the CB2001 predicts lower in-plane yield stress values

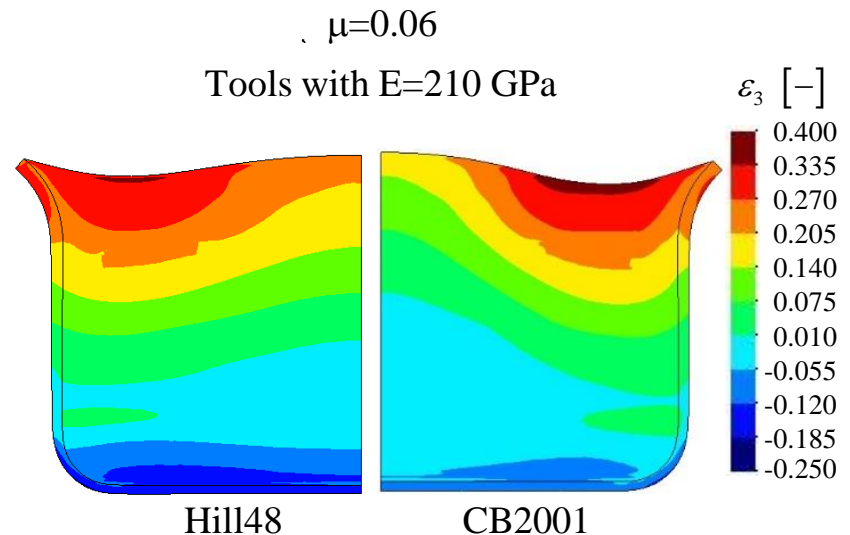
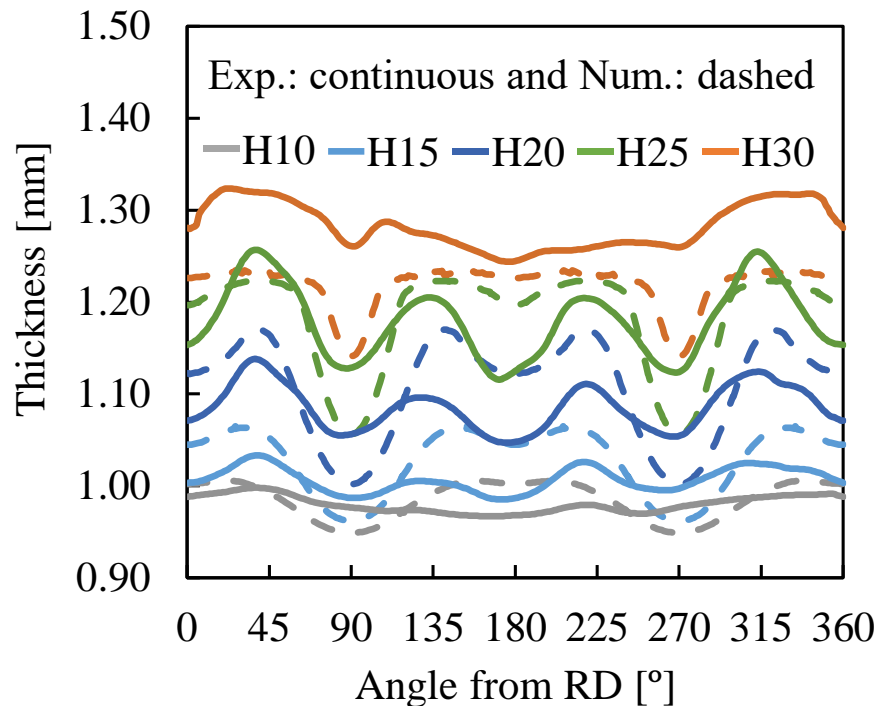


Comparison between experimental and predicted results considering deformable tools and evolutionary friction with the Hill'48 and the CB2001 yield criteria: (a) punch force-displacement and (b) earing profile.

Results and discussion

Deformable tools: yield criteria

- The thickness strain is dictated by the normal to the yield surface in the region between uniaxial compression and pure shear stress states, which were not covered by the experimental tests performed



Comparison between experimental and predicted results considering deformable tools and an evolutionary friction coefficient: (left) distribution of the thickness along the cup circumference at different heights with the CB2001 yield criteria and (right) contour plot of the thickness strain for a punch displacement of 35 mm.

Conclusions

- The **tools stiffness** affects the thickness average value, at each height, but also the trend along the circumferential direction, due to the **orthotropic behaviour of the blank**, which imposes a different thickening of the flange.
- Higher thickening values, associated with lower r -values, result in higher contact pressures and, consequently, higher radial displacement of the tools.
- An evolutionary friction law is required to enable capturing **both the drawing and ironing forces**.
- There is an **interaction** between the tools stiffness and the friction law.
- The thickness distribution at the end of the ironing stage is dictated by the one predicted at the end of the drawing stage, which requires improved knowledge about the **direction of the plastic strain-rate in the compression-tension quadrant**.

Acknowledgements

The authors gratefully acknowledge the financial support of the Portuguese Foundation for Science and Technology (FCT) under projects with reference PTDC/EME-EME/30592/2017 and PTDC/EME-EME/31657/2017 and by European Regional Development Fund (ERDF) through the Portugal 2020 program and the Centro 2020 Regional Operational Programme (CENTRO-01-0145-FEDER-031657) under the project UIDB/00285/2020.

Projetos Cofinanciados pela UE:

